

Higgs boson decay to massive bottom quarks at order α_s^4 induced by top-quark Yukawa couplings

Jian Wang^{1,2}, Xing Wang³, and Yefan Wang^{4,5}

¹School of Physics, Shandong University, Jinan, Shandong 250100, China

²Center for High Energy Physics, Peking University, Beijing 100871, China

³School of Science and Engineering, The Chinese University of Hong Kong, Shenzhen, Longgang, 518172 Shenzhen, China

⁴Department of Physics and Institute of Theoretical Physics, Nanjing Normal University, Nanjing, Jiangsu 210023, China

⁵Nanjing Key Laboratory of Particle Physics and Astrophysics, Nanjing Normal University, Nanjing, Jiangsu 210023, China

March 20, 2026

Abstract

The Higgs boson decay to massive bottom quarks has the largest branching ratio. The decay is mainly induced by the bottom-quark Yukawa coupling with the decay rate calculated up to $\mathcal{O}(\alpha_s^4)$ assuming the massless final-state bottom quark. The top-quark Yukawa coupling induced contribution starts at $\mathcal{O}(\alpha_s^2)$, and exhibits logarithmic and power enhancements, making the perturbative expansion converge slowly. We present a calculation of such contributions at $\mathcal{O}(\alpha_s^4)$ to the decay into massive bottom quarks in which the squared amplitudes contain two top-quark Yukawa couplings. We find that they increase the decay width, relative to the result up to $\mathcal{O}(\alpha_s^3)$, by 0.4%, larger than the experimental precision at future lepton colliders, and reduce the scale dependence significantly down to 0.4%.

1 Introduction

The decay of the Higgs boson into a bottom–antibottom quark pair, $H \rightarrow b\bar{b}$, is the dominant channel in the Standard Model (SM), governing the Higgs boson total width and providing a direct probe of the bottom-quark Yukawa coupling. Precision measurements of this coupling, projected to reach the percent or even subpercent level at future colliders such as the HL-LHC [1] and a potential e^+e^- Higgs factory [2–4], necessitate a theoretical prediction with matching precision. The primary source of theoretical uncertainty stems from higher-order Quantum Chromodynamics (QCD) corrections, which are substantial due to the large strong coupling constant at the relevant scale and the emergence of high-energy logarithms.

A systematic perturbative expansion is essential for a reliable prediction. The calculation of this decay width has a long history, with the next-to-leading order (NLO) QCD and electroweak (EW) corrections established thirty years ago [5–10]. The next-to-next-to-leading order (NNLO) QCD corrections were calculated for the total and differential decay rate in [11–14] and [15–17], respectively. Even higher order QCD corrections were obtained assuming that the final-state bottom quark is massless [18–27]. Simultaneously, the mixed QCD×EW corrections were computed in [28, 29]. Recently, the top quark induced contribution has been investigated at $\mathcal{O}(\alpha_s^2)$ [13] and $\mathcal{O}(\alpha_s^3)$ [30, 31], respectively. The calculation in [31] was performed within an effective field theory framework, integrating out the top quark, and decomposing the width into contributions from different effective operator combinations: C_2C_2 (pure bottom Yukawa), C_1C_2 (interference), and C_1C_1 (pure gluonic), where C_i are the Wilson coefficients of the effective operators. For the dominant C_2C_2 contribution, corrections beyond NNLO were found to be below 0.2% when assuming massless final-state b -quarks [20, 21]. However, the C_1C_2 interference term, induced by the top-quark Yukawa coupling, exhibits a markedly different behaviour. It is enhanced by large logarithmic terms $\log^j(m_H^2/m_b^2)$ with $j = 1, 2$ already at $\mathcal{O}(\alpha_s^2)$, and at $\mathcal{O}(\alpha_s^3)$ it includes terms with up to $\log^4(m_H^2/m_b^2)$. These logarithms, originating from soft massive quark effects at subleading power, are not Sudakov-like and are characterised by a distinct colour structure proportional to $C_A - C_F$. Although the C_1C_1 contribution appears firstly at $\mathcal{O}(\alpha_s^3)$, it is power enhanced with respect to the C_2C_2 and C_1C_2 terms. Consequently, the N³LO corrections increase the NNLO result by approximately 1%, significantly exceeding naive α_s power-counting expectations [31]. This underscores the importance of a full analytic treatment of finite b -quark mass effects in the top-induced contribution for precise phenomenology.

With the N³LO calculation complete, the logical next step is the computation of the fourth-order (N⁴LO) corrections. This advancement is crucial for several reasons. First, it will further reduce the residual renormalization scale dependence, which remains one of the dominant theoretical uncertainties at N³LO. Second, it provides a decisive test of the convergence of the perturbative series at an unprecedented level. Third, it probes the higher-order structure of the soft massive quark logarithms that appear in the C_1C_2 and C_1C_1 channels, offering essential data for developing all-order resummation formalisms at subleading power.

Since the bottom quark mass effect is negligible in the C_2C_2 channel, it is reasonable to take the result in refs. [20, 21] with massless bottom quarks. In this paper, as an extension of our previous works [14, 31, 32], we present an analytic result of the $\mathcal{O}(\alpha_s^4)$ correction in the C_1C_1 channel with full dependence on the bottom quark mass, leaving the calculation of the C_1C_2 channel to future work.

This paper is organized as follows. In section 2, we describe the framework to perform the calculation, including the effective operators and the decomposition of the decay width into different channels. The MIs needed in the amplitude of $H \rightarrow b\bar{b} \rightarrow H$ are calculated analytically in section 3, while the numerical results of the decay width are provided in section 4. We conclude in section 5.

2 Calculation framework

In calculation of the decay rate of $H \rightarrow b\bar{b}$, we adopt the effective Lagrangian

$$\mathcal{L}_{\text{eff}} = -\frac{H}{v} (C_1 \mathcal{O}_1^R + C_2 \mathcal{O}_2^R) + \mathcal{L}_{\text{QCD}}, \quad (1)$$

where v is the vacuum expectation value of the Higgs field H and \mathcal{L}_{QCD} is the QCD Lagrangian with the top quark decoupled. The two renormalized effective operators are defined by

$$\mathcal{O}_1^R = Z_{11} \mathcal{O}_1 + Z_{12} \mathcal{O}_2, \quad \mathcal{O}_2^R = Z_{21} \mathcal{O}_1 + Z_{22} \mathcal{O}_2 \quad (2)$$

with

$$\mathcal{O}_1 = (G_{a,\mu\nu}^0)^2, \quad \mathcal{O}_2 = m_b^0 \bar{b}^0 b^0. \quad (3)$$

Here the superscript ‘‘0’’ indicates that the fields and couplings are bare quantities. The mixing between these two effective operators is described by the renormalization constants Z_{ij} , which are given by [33–37],

$$\begin{aligned} Z_{11} &= 1 + \alpha_s \frac{\partial \log Z_{\alpha_s}}{\partial \alpha_s} = 1 + \left(\frac{\alpha_s}{\pi}\right) \left(\frac{-11C_A + 2n_f}{12\epsilon}\right) \\ &\quad + \left(\frac{\alpha_s}{\pi}\right)^2 \left(\frac{(-11C_A + 2n_f)^2}{144\epsilon^2} - \frac{17C_A^2 - 5C_A n_f - 3C_F n_f}{24\epsilon}\right) + \mathcal{O}(\alpha_s^3), \\ Z_{12} &= -4\alpha_s \frac{\partial \log Z_m^{\overline{\text{MS}}}}{\partial \alpha_s} = \left(\frac{\alpha_s}{\pi}\right) \left(\frac{3C_F}{\epsilon}\right) \\ &\quad + \left(\frac{\alpha_s}{\pi}\right)^2 C_F \left(\frac{-11C_A + 2n_f}{4\epsilon^2} + \frac{97C_A + 9C_F - 10n_f}{24\epsilon}\right) + \mathcal{O}(\alpha_s^3), \\ Z_{21} &= 0, \\ Z_{22} &= 1, \end{aligned} \quad (4)$$

where $C_A = 3$ and $C_F = 4/3$ in QCD and $n_f = 5$. The top quark effect is encoded in the Wilson coefficients [36–40],

$$\begin{aligned} C_1 &= -\left(\frac{\alpha_s}{\pi}\right) \frac{1}{12} - \left(\frac{\alpha_s}{\pi}\right)^2 \frac{11}{48} - \left(\frac{\alpha_s}{\pi}\right)^3 \left[\frac{137}{576} L_t + \frac{443}{864}\right] + \mathcal{O}(\alpha_s^4), \\ C_2 &= 1 + \left(\frac{\alpha_s}{\pi}\right)^2 \left[-\frac{1}{3} L_t + \frac{5}{18}\right] + \left(\frac{\alpha_s}{\pi}\right)^3 \left[-\frac{23}{36} L_t^2 - \frac{79}{36} L_t + \frac{749}{1296} + \frac{5}{3} \zeta(3)\right] \\ &\quad + \left(\frac{\alpha_s}{\pi}\right)^4 \left[-\frac{529}{432} L_t^3 - \frac{1093}{144} L_t^2 + \frac{55\zeta(3)}{4} L_t - \frac{14045}{864} L_t - \frac{575\zeta(5)}{36} + \frac{14}{3} \text{Li}_4\left(\frac{1}{2}\right)\right. \\ &\quad \left. - \frac{277\pi^4}{1440} - \frac{7\pi^2 \log^2(2)}{36} + \frac{7 \log^4(2)}{36} + \frac{30773\zeta(3)}{1536} - \frac{2\pi^2 \log(2)}{27} - \frac{\pi^2}{27} + \frac{198665}{62208}\right] + \mathcal{O}(\alpha_s^5), \end{aligned} \quad (5)$$

where $L_t = \log(\mu^2/m_t^2)$ and m_t is the on-shell top quark mass. The $1/m_t^2$ higher power corrections in the decay width of $H \rightarrow b\bar{b}$ start at $\mathcal{O}(\alpha_s^2)$, modifying the $\mathcal{O}(\alpha_s^2)$ correction by only 0.1% [13], and thus can be fully neglected in the decay width.

The decay amplitude of $H \rightarrow b\bar{b}$ can be induced by either of the effective operators and thus the decay width can be decomposed as

$$\Gamma_{H \rightarrow b\bar{b}} = \Gamma_{H \rightarrow b\bar{b}}^{C_2 C_2} + \Gamma_{H \rightarrow b\bar{b}}^{C_1 C_2} + \Gamma_{H \rightarrow b\bar{b}}^{C_1 C_1}. \quad (6)$$

The superscripts denote the combination structure of effective operators in the squared amplitudes. Each term in the above equation can be expanded in the strong coupling α_s ,

$$\Gamma_{H \rightarrow b\bar{b}}^{C_2 C_2} = C_2 C_2 \left[\Delta_{0,b\bar{b}}^{C_2 C_2} + \left(\frac{\alpha_s}{\pi}\right) \Delta_{1,b\bar{b}}^{C_2 C_2} + \left(\frac{\alpha_s}{\pi}\right)^2 \Delta_{2,b\bar{b}}^{C_2 C_2} + \left(\frac{\alpha_s}{\pi}\right)^3 \Delta_{3,b\bar{b}}^{C_2 C_2} + \left(\frac{\alpha_s}{\pi}\right)^4 \Delta_{4,b\bar{b}}^{C_2 C_2} + \mathcal{O}(\alpha_s^5) \right],$$

$$\begin{aligned}\Gamma_{H\rightarrow b\bar{b}}^{C_1 C_2} &= C_1 C_2 \left[\left(\frac{\alpha_s}{\pi}\right) \Delta_{1,b\bar{b}}^{C_1 C_2} + \left(\frac{\alpha_s}{\pi}\right)^2 \Delta_{2,b\bar{b}}^{C_1 C_2} + \left(\frac{\alpha_s}{\pi}\right)^3 \Delta_{3,b\bar{b}}^{C_1 C_2} + \mathcal{O}(\alpha_s^4) \right], \\ \Gamma_{H\rightarrow b\bar{b}}^{C_1 C_1} &= C_1 C_1 \left[\left(\frac{\alpha_s}{\pi}\right) \Delta_{1,b\bar{b}}^{C_1 C_1} + \left(\frac{\alpha_s}{\pi}\right)^2 \Delta_{2,b\bar{b}}^{C_1 C_1} + \mathcal{O}(\alpha_s^3) \right],\end{aligned}\quad (7)$$

where we have shown explicitly the terms needed to obtain $\Gamma_{H\rightarrow b\bar{b}}$ to $\mathcal{O}(\alpha_s^4)$. Notice that the leading order contributions of $\Gamma_{H\rightarrow b\bar{b}}^{C_1 C_2}$ and $\Gamma_{H\rightarrow b\bar{b}}^{C_1 C_1}$ are $\mathcal{O}(\alpha_s^2)$ and $\mathcal{O}(\alpha_s^3)$, respectively.

The results of $\Delta_{i,b\bar{b}}^{C_2 C_2}$ have been obtained up to $\mathcal{O}(\alpha_s^4)$ with massless final-state bottom quarks [18–21]. Defining $z \equiv m_H^2/m_b^2$, they are given by

$$\begin{aligned}\Delta_{0,b\bar{b}}^{C_2 C_2}|_{z\rightarrow\infty} &= \frac{3m_H\bar{m}_b(m_H)^2}{8v^2\pi} + \mathcal{O}(z^{-1}), \\ \Delta_{1,b\bar{b}}^{C_2 C_2}|_{z\rightarrow\infty} &= \frac{17m_H\bar{m}_b(m_H)^2}{8v^2\pi} + \mathcal{O}(z^{-1}), \\ \Delta_{2,b\bar{b}}^{C_2 C_2}|_{z\rightarrow\infty} &= \frac{m_H\bar{m}_b(m_H)^2}{96v^2\pi} \left[-582\zeta(3) - 47\pi^2 + \frac{8851}{4} \right] + \mathcal{O}(z^{-1}), \\ \Delta_{3,b\bar{b}}^{C_2 C_2}|_{z\rightarrow\infty} &= \frac{m_H\bar{m}_b(m_H)^2}{96v^2\pi} \left[1945\zeta(5) - \frac{5\pi^4}{3} - \frac{80095\zeta(3)}{6} - \frac{10225\pi^2}{9} + \frac{34873057}{1296} \right] + \mathcal{O}(z^{-1}), \\ \Delta_{4,b\bar{b}}^{C_2 C_2}|_{z\rightarrow\infty} &= \frac{m_H\bar{m}_b(m_H)^2}{96v^2\pi} \left[-\frac{427735\zeta(7)}{64} + \frac{50\pi^6}{189} + \frac{84625\zeta(3)^2}{3} + \frac{469675\zeta(5)}{12} + \frac{116945\pi^2\zeta(3)}{24} \right. \\ &\quad \left. + \frac{667\pi^4}{8} - \frac{12308897\zeta(3)}{48} - \frac{19637651\pi^2}{864} + \frac{5005075879}{13824} \right] + \mathcal{O}(z^{-1}).\end{aligned}\quad (8)$$

The analytical result with full bottom-quark mass dependence at $\mathcal{O}(\alpha_s^2)$ was obtained in [14], showing that the $\mathcal{O}(z^{-1})$ power correction is below 1% relative to the leading power result. This is because the expansion parameter is rather small ($z^{-1} \approx 0.1\%$) and no logarithmic or power enhancement, such as $\log(z)$ or z , exists in the result. Similar corrections are expected at higher orders and thus completely negligible.

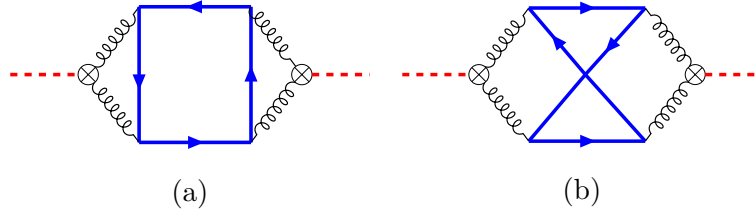


Figure 1: Sample three-loop Feynman diagrams contributing to $\Delta_{2,b\bar{b}}^{C_1 C_1}$. The thick blue and dashed red lines denote the massive bottom quark and the Higgs boson, respectively.

The full analytic results of $\Delta_{i,b\bar{b}}^{C_1 C_2}$ with $i = 1, 2$ can be found in Ref. [31]. In the small m_b limit, $\Delta_{1,b\bar{b}}^{C_1 C_2}$ reads

$$\begin{aligned}\Delta_{1,b\bar{b}}^{C_1 C_2}|_{z\rightarrow\infty} &= \frac{4m_H m_b \bar{m}_b(\mu)}{\pi v^2} \left[-\frac{1}{8} \log^2(z) - \frac{3}{4} \log\left(\frac{\mu^2}{m_H^2}\right) + \frac{\pi^2}{8} - \frac{19}{8} \right. \\ &\quad \left. + \frac{1}{2} \frac{\log^2(z)}{z} + 2 \frac{\log(z)}{z} + \frac{9}{2z} \log\left(\frac{\mu^2}{m_H^2}\right) - \frac{\pi^2}{2z} + \frac{15}{2z} \right] + \mathcal{O}(z^{-2}).\end{aligned}\quad (9)$$

The expression of $\Delta_{2,b\bar{b}}^{C_1 C_2}$ is too lengthy to be shown here. A prominent feature is that it contains logarithmic terms up to $\log^4(z)$. So far, a calculation of $\Delta_{3,b\bar{b}}^{C_1 C_2}$, either analytical or numerical, is still missing.

The analytic result of $\Delta_{1,b\bar{b}}^{C_1C_1}$ has also been known in [31], and the asymptotic form is

$$\Delta_{1,b\bar{b}}^{C_1C_1}|_{z \rightarrow \infty} = \frac{4m_H^3}{\pi v^2} \left[\frac{1}{6} \log(z) - \frac{7}{12} + \frac{3}{z} \right] + \mathcal{O}(z^{-2}). \quad (10)$$

It can be seen that this contribution is power enhanced compared to the results of $\Delta_{i,b\bar{b}}^{C_2C_2}$. In this work, we focus on the contribution of $\Gamma_{H \rightarrow b\bar{b}}^{C_1C_1}$ at $\mathcal{O}(\alpha_s^4)$, then we need to calculate $\Delta_{2,b\bar{b}}^{C_1C_1}$. We perform the calculation using the optical theorem, i.e.,

$$\Gamma_{H \rightarrow b\bar{b}} = \frac{\text{Im}_{b\bar{b}}(\Sigma)}{m_H}, \quad (11)$$

where Σ represents the amplitude of $H \rightarrow b\bar{b} \rightarrow H$. Specifically, $\Delta_{2,b\bar{b}}^{C_1C_1}$ corresponds to the three-loop Feynman diagrams which contain two \mathcal{O}_1 vertices. Typical diagrams can be seen in figure 1. The notation $\text{Im}_{b\bar{b}}$ in eq. (11) indicates that the imaginary part is taken only for the cut on at least one bottom quark pair. Explicitly, $\Delta_{2,b\bar{b}}^{C_1C_1}$ can be divided into two parts

$$\Delta_{2,b\bar{b}}^{C_1C_1} = \tilde{\Delta}_{2,b\bar{b}}^{C_1C_1} + \Delta_{2,b\bar{b}\bar{b}\bar{b}}^{C_1C_1}, \quad (12)$$

where $\tilde{\Delta}_{2,b\bar{b}}^{C_1C_1}$ represents the contribution from the final states of $b\bar{b}$, $b\bar{b}g$, $b\bar{b}gg$, and $b\bar{b}q\bar{q}$, while $\Delta_{2,b\bar{b}\bar{b}\bar{b}}^{C_1C_1}$ receives contributions from the final state of $b\bar{b}\bar{b}\bar{b}$.

The Feynman diagrams are generated using the package `FeynArts` [41] with effective vertices being implemented via `FeynRules` [42]. The corresponding amplitudes are simplified with the package `FeynCalc` [43, 44] and expressed as a linear combination of scalar integrals. They are reduced to a set of basis integrals called master integrals (MIs) using the integration by parts (IBP) identities [45, 46] with the help of the package `Kira` [47].

3 Analytic calculation of MIs

We find that the MIs belong to one integral family, which is defined by

$$I_{n_1, n_2, \dots, n_9} = \text{Im}_{b\bar{b}} \int \prod_{i=1}^3 \frac{(m_b^2)^\epsilon d^{4-2\epsilon} q_i}{i\pi^{2-\epsilon} \Gamma(1+\epsilon)} \frac{1}{D_1^{n_1} D_2^{n_2} D_3^{n_3} D_4^{n_4} D_5^{n_5} D_6^{n_6} D_7^{n_7} D_8^{n_8} D_9^{n_9}}, \quad (13)$$

with all n_i being integers. The denominators D_i are defined as

$$\begin{aligned} D_1 &= q_1^2, & D_2 &= (q_1 - q_2)^2 - m_b^2, & D_3 &= q_2^2 - m_b^2, \\ D_4 &= q_3^2, & D_5 &= (q_2 + q_3)^2 - m_b^2, & D_6 &= (q_3 - k)^2 - m_b^2, \\ D_7 &= (q_1 + k)^2, & D_8 &= (q_1 - q_2 - q_3 + k)^2, & D_9 &= (q_1 - q_2 - q_3)^2 - m_b^2, \end{aligned} \quad (14)$$

where the momentum of the Higgs boson satisfies $k^2 = m_H^2$. There are 38 MIs (M_1 - M_{38}) appearing in the calculations of amplitudes. The corresponding topological diagrams are shown in appendix A. Similar to eq. (12), the MIs can be divided into two parts,

$$M_i = \tilde{M}_{i,b\bar{b}} + M_{i,4b}, \quad (15)$$

where $\tilde{M}_{i,b\bar{b}}$ and $M_{i,4b}$ contribute to $\tilde{\Delta}_{2,b\bar{b}}^{C_1C_1}$ and $\Delta_{2,b\bar{b}\bar{b}\bar{b}}^{C_1C_1}$, respectively.

We find that M_1 - M_{35} have been analytically calculated in our previous works [14, 31, 48]. Most of these MIs can contribute to $\tilde{\Delta}_{2,b\bar{b}}^{C_1C_1}$ except for the first three MIs (banana diagrams at three loops), which only contain cuts on $b\bar{b}\bar{b}\bar{b}$, i.e.,

$$\tilde{M}_{1,b\bar{b}} = \tilde{M}_{2,b\bar{b}} = \tilde{M}_{3,b\bar{b}} = 0. \quad (16)$$

Since $M_{1,4b}$ - $M_{3,4b}$, containing elliptic integrals, serve as the lower sector of the other $M_{i,4b}$, all $M_{i,4b}$ are consequently related to the elliptic integrals. Fortunately, $\Delta_{2,bbb\bar{b}}^{C_1C_1}$ is finite as it corresponds to the interference of tree-level diagrams for $H \rightarrow b\bar{b}b\bar{b}$. By adopting a regular basis in [49], only the $\mathcal{O}(\epsilon^0)$ parts are required in the amplitude calculations. Finally, all $M_{i,4b}$ ($i = 1, \dots, 35$) can be expressed either as complete elliptic integrals of the first kind or as one-fold integrals of them. The integrals $\tilde{M}_{i,b\bar{b}}$ ($i = 1, \dots, 35$) can be solved by constructing canonical differential equations [50, 51]. In this procedure, there are two square roots

$$r_1 = \sqrt{z(z-4)}, \quad r_2 = \sqrt{z(z+4)}. \quad (17)$$

The variable redefinition

$$z = -\frac{(w-1)^2}{w}, \quad -1 < w < 0 \quad (18)$$

can rationalize r_1 while

$$z = -\frac{(y^2+1)^2}{(y-1)y(y+1)}, \quad 0 < y < \sqrt{2}-1 \quad (19)$$

can rationalize both r_1 and r_2 . In this way, all the $\tilde{M}_{i,b\bar{b}}$ ($i = 1, \dots, 35$) can be solved recursively, yielding analytic results expressed as linear combinations of multiple polylogarithms (MPLs) [52]. The boundary conditions are fixed by the PSLQ algorithm [53] together with the high-precision numerical results obtained from the package `AMFlow` [54–57].

M_{36} - M_{38} are the new MIs to be computed,

$$M_{36} = I_{1,1,0,1,1,1,1,1,1}, \quad M_{37} = I_{1,1,1,1,1,1,1,1,0}, \quad M_{38} = I_{1,1,1,1,1,1,1,2,0}. \quad (20)$$

M_{36} only contributes to $\tilde{\Delta}_{2,b\bar{b}}^{C_1C_1}$, i.e., $M_{36,4b} = 0$. We find that $(1-2\epsilon)\epsilon^5 m_b^4 r_1 z M_{36}$ forms a dimensionless canonical basis, which can be expressed in terms of MPLs using the variable y .

We now turn to the top sector consisting of M_{37} and M_{38} . These two MIs contribute to both $\tilde{\Delta}_{2,b\bar{b}}^{C_1C_1}$ and $\Delta_{2,bbb\bar{b}}^{C_1C_1}$. In both cases, they are finite, and thus only their $\mathcal{O}(\epsilon^0)$ parts are required. Accordingly, we define

$$\begin{aligned} F_{37,b\bar{b}} &= z^2 m_b^4 \tilde{M}_{37,b\bar{b}}|_{\epsilon=0}, & F_{38,b\bar{b}} &= z^2 m_b^6 \tilde{M}_{38,b\bar{b}}|_{\epsilon=0}, \\ F_{37,4b} &= z^2 m_b^4 M_{37,4b}|_{\epsilon=0}, & F_{38,4b} &= z^2 m_b^6 M_{38,4b}|_{\epsilon=0}. \end{aligned} \quad (21)$$

These basis integrals satisfy the differential equations

$$\begin{aligned} \frac{\partial F_{37,b\bar{b}}(4b)}{\partial z} &= -\frac{4F_{38,b\bar{b}}(4b)}{z}, \\ \frac{\partial F_{38,b\bar{b}}(4b)}{\partial z} &= \frac{F_{37,b\bar{b}}(4b)}{z(z+16)} + \frac{16F_{38,b\bar{b}}(4b)}{z(z+16)} + R_{b\bar{b}}(4b)(z), \end{aligned} \quad (22)$$

where the homogeneous parts are the same for the $b\bar{b}$ and $4b$ cuts. The only difference is represented by $R_{b\bar{b}}(4b)(z)$, which is fully determined by the MIs in lower sectors. Their solutions can be written as one-fold integrals:

$$\begin{aligned} F_{37,b\bar{b}}(z) &= \int_4^z \frac{(K(-\frac{x}{16})K(\frac{z+16}{16}) - K(\frac{x+16}{16})K(-\frac{z}{16}))(x+16)\sqrt{z}}{\pi\sqrt{x}} R_{b\bar{b}}(x) dx, \\ F_{38,b\bar{b}}(z) &= \int_4^z \frac{2(K(\frac{x+16}{16})E(-\frac{z}{16}) + K(-\frac{x}{16})(E(\frac{z+16}{16}) - K(\frac{z+16}{16}))) (x+16)\sqrt{z}}{\pi(z+16)\sqrt{x}} R_{b\bar{b}}(x) dx, \end{aligned} \quad (23)$$

and similarly

$$F_{37,4b}(z) = \int_{16}^z \frac{(K(-\frac{x}{16})K(\frac{z+16}{16}) - K(\frac{x+16}{16})K(-\frac{z}{16})) (x+16)\sqrt{z}}{\pi\sqrt{x}} R_{4b}(x) dx, \quad (24)$$

$$F_{38,4b}(z) = \int_{16}^z \frac{2(K(\frac{x+16}{16})E(-\frac{z}{16}) + K(-\frac{x}{16})(E(\frac{z+16}{16}) - K(\frac{z+16}{16}))) (x+16)\sqrt{z}}{\pi(z+16)\sqrt{x}} R_{4b}(x) dx,$$

where K and E are the complete elliptic integrals of the first and second kinds, respectively. The distinctions between $F_{i,b\bar{b}}(z)$ and $F_{i,4b}(z)$ lie in the lower integration limits and the specific forms of $R(x)$. It can be seen that these integrals vanish at the threshold, i.e., $z = 4(16)$ for $F_{i,b\bar{b}}(z)$ ($F_{i,4b}(z)$). For the $b\bar{b}$ final state, $R_{b\bar{b}}$ is the linear combination of logarithmic and Li_2 functions, so the final results of $F_{i,b\bar{b}}(z)$ are expressed as one-fold integrals. For the $b\bar{b}b\bar{b}$ final state, however, R_{4b} itself is already a one-fold integral [49]. Consequently, the final expressions of $F_{i,4b}(z)$ take the form of two-fold integrals.

The above integral representation can be numerically evaluated. In addition, we can derive the asymptotic form in the small m_b ($z \rightarrow \infty$) limit,

$$F_{37,b\bar{b}}|_{z \rightarrow \infty} = -\frac{11\pi}{6} \log^4(z) + \frac{31\pi^3}{3} \log^2(z) - 128\pi\zeta(3) \log(z) - \frac{323\pi^5}{90} + \mathcal{O}(z^{-1}),$$

$$F_{38,b\bar{b}}|_{z \rightarrow \infty} = \frac{11\pi}{6} \log^3(z) - \frac{31\pi^3}{6} \log(z) + 32\pi\zeta(3) + \mathcal{O}(z^{-1}),$$

$$F_{37,4b}|_{z \rightarrow \infty} = \frac{7\pi}{6} \log^4(z) - \frac{13\pi^3}{3} \log^2(z) + 48\pi\zeta(3) \log(z) + \frac{181\pi^5}{90} + \mathcal{O}(z^{-1}),$$

$$F_{38,4b}|_{z \rightarrow \infty} = -\frac{7\pi}{6} \log^3(z) + \frac{13\pi^3}{6} \log(z) - 12\pi\zeta(3) + \mathcal{O}(z^{-1}). \quad (25)$$

Before proceeding, we comment on another method to compute the MIs. We have constructed the ϵ -factorised differential equations for all master integrals, including the banana integrals and the above top sector, which is elliptic by itself, and solved them beyond leading orders in ϵ . We find full agreement between these two methods. The details will be presented in a forthcoming paper [58], and the upshot is as follows. Firstly, the solutions in expansions of ϵ are straightforward to obtain and do not involve one-fold or two-fold integrals. Secondly, this integral family, and hence the physical observable, incorporates several geometric objects in a non-trivial way. Consequently, it is a practical application of the algorithm to find the ϵ -factorised differential equation proposed recently in [59, 60], including mixing between different sectors. On top of that, since all the integrals involve only one dimensionless variable z , it is potentially a good playground to investigate how different geometries talk to each other at the observable level.

After computing the MIs, we can obtain the analytical results for the decay width, which are provided in the auxiliary file. Here, we only present the asymptotic form:

$$\begin{aligned} \tilde{\Delta}_{2,b\bar{b}}^{C_1 C_1}|_{z \rightarrow \infty} &= \frac{m_H^3}{\pi v^2} \times \\ &\left(C_A C_F^2 \left[\frac{\log(z)}{8} + \frac{\zeta(3)}{3} - \frac{29}{96} - \frac{\log^4(z)}{96z} + \frac{\log^3(z)}{8z} + \frac{3}{8} \log\left(\frac{\mu^2}{m_H^2}\right) \frac{\log^2(z)}{z} \right. \right. \\ &\quad \left. \left. - \frac{\pi^2 \log^2(z)}{48z} + \frac{3 \log^2(z)}{8z} + \frac{5\zeta(3) \log(z)}{2z} + \frac{13\pi^2 \log(z)}{24z} - \frac{41 \log(z)}{8z} \right. \right. \\ &\quad \left. \left. + \frac{9}{8z} \log^2\left(\frac{\mu^2}{m_H^2}\right) - \frac{3\pi^2}{8z} \log\left(\frac{\mu^2}{m_H^2}\right) + \frac{57}{8z} \log\left(\frac{\mu^2}{m_H^2}\right) + \frac{3\pi^4}{160z} - \frac{15\zeta(3)}{2z} - \frac{7\pi^2}{12z} + \frac{237}{16z} \right] \right. \\ &\quad \left. + C_A^2 C_F \left[\frac{\log^3(z)}{72} - \frac{5 \log^2(z)}{72} - \frac{\pi^2}{18} \log(z) + \frac{11}{24} \log\left(\frac{\mu^2}{m_H^2}\right) \log(z) + \frac{859 \log(z)}{432} \right. \right. \\ &\quad \left. \left. - \frac{77}{48} \log\left(\frac{\mu^2}{m_H^2}\right) + \frac{\zeta(3)}{4} + \frac{53\pi^2}{216} - \frac{4897}{648} + \frac{\log^3(z)}{12z} + \frac{3 \log^2(z)}{4z} - \frac{7\pi^2 \log(z)}{24z} \right] \right) \end{aligned}$$

$$\begin{aligned}
& + \frac{\log(z)}{8z} + \frac{33}{4z} \log\left(\frac{\mu^2}{m_H^2}\right) + \frac{4\zeta(3)}{z} - \frac{11\pi^2}{12z} + \frac{457}{16z} \Big] \\
& + C_A C_F n_l \left[-\frac{\log^2(z)}{36} - \frac{7\log(z)}{72} - \frac{1}{12} \log\left(\frac{\mu^2}{m_H^2}\right) \log(z) + \frac{7}{24} \log\left(\frac{\mu^2}{m_H^2}\right) \right. \\
& + \left. \frac{455}{648} - \frac{\log(z)}{z} - \frac{3}{2z} \log\left(\frac{\mu^2}{m_H^2}\right) - \frac{9}{4z} \right] \\
& + C_A C_F \left[-\frac{\log^2(z)}{18} + \frac{7\log(z)}{72} - \frac{1}{12} \log\left(\frac{\mu^2}{m_H^2}\right) \log(z) + \frac{7}{24} \log\left(\frac{\mu^2}{m_H^2}\right) - \frac{\pi^2}{108} \right. \\
& + \left. \frac{245}{648} - \frac{\log(z)}{2z} - \frac{3}{2z} \log\left(\frac{\mu^2}{m_H^2}\right) - \frac{13}{6z} \right] + \mathcal{O}(z^{-2}), \tag{26}
\end{aligned}$$

and

$$\begin{aligned}
\Delta_{2,b\bar{b}b\bar{b}}^{C_1 C_1} |_{z \rightarrow \infty} &= \frac{m_H^3}{\pi v^2} \times \\
& \left((2C_A C_F^2 - C_A^2 C_F) \left[\frac{5}{96} - \frac{\zeta(3)}{24} + \frac{\log^2(z)}{16z} - \frac{3\log(z)}{16z} - \frac{\pi^2}{16z} + \frac{7}{32z} \right] \right. \\
& + \left. C_A C_F \left[\frac{\log^2(z)}{72} - \frac{7\log(z)}{72} - \frac{\pi^2}{216} + \frac{17}{81} + \frac{\log(z)}{2z} - \frac{19}{12z} \right] \right) + \mathcal{O}(z^{-2}). \tag{27}
\end{aligned}$$

In fact, these asymptotic results are accurate enough for phenomenological studies since the omitted higher-power terms introduce a correction of less than 0.1%. The above results are given in terms of the on-shell mass m_b . They can be converted to the $\overline{\text{MS}}$ scheme via the relation

$$\overline{m}_b(\mu) = m_b \left(1 - \left(\frac{\alpha_s}{\pi} \right) C_F \left[1 + \frac{3}{4} \log\left(\frac{\mu^2}{m_b^2}\right) \right] + \mathcal{O}(\alpha_s^2) \right). \tag{28}$$

Compared to the contributions induced by the bottom quark Yukawa coupling in eq. (8), $\tilde{\Delta}_{2,b\bar{b}}^{C_1 C_1}$ and $\Delta_{2,b\bar{b}b\bar{b}}^{C_1 C_1}$ are power enhanced. This feature has been previously observed in the calculation of $\Delta_{1,b\bar{b}}^{C_1 C_1}$ [31]; see eq. (10). The ratio of the leading logarithms of $\Delta_{2,b\bar{b}}^{C_1 C_1}$ over that of $\Delta_{1,b\bar{b}}^{C_1 C_1}$ is

$$\frac{1}{12} C_A \log^2(z) \tag{29}$$

at the leading power and

$$-\frac{1}{288} C_F \log^4(z) \tag{30}$$

at the subleading power. The distinct color structures and powers indicate that they have different origins. The double-logarithmic enhancement arises from the diagram with a gluon splitting into a bottom-quark pair, while the quartic term appears in the diagram featuring exchanges of two soft bottom quarks. Similar enhancements have been found in the calculation of $\mathcal{O}(\alpha_s^2)$ corrections in the $C_2 C_2$ channel with $b\bar{b}$ cut [14] (see figure 8 there). The behaviour of such large logarithms at all orders is very interesting and deserves a detailed study in the future.

4 Numerical results

To present the numerical results for the decay width of $H \rightarrow b\bar{b}$, we adopt the following input parameters [61, 62]:

$$\overline{m}_b(\overline{m}_b) = 4.18 \text{ GeV}, \quad m_H = 125.09 \text{ GeV}, \quad m_t = 172.57 \text{ GeV},$$

$$\alpha_s(m_Z) = 0.1180 \pm 0.0009, \quad G_F = 1.166378 \times 10^{-5} \text{ GeV}^{-2}. \quad (31)$$

\overline{m}_b at other scales is evaluated with the package RunDec [63, 64], e.g., $\overline{m}_b(m_H/2) = 2.959 \text{ GeV}$, $\overline{m}_b(m_H) = 2.787 \text{ GeV}$ and $\overline{m}_b(2m_H) = 2.642 \text{ GeV}$. The running strong coupling at the typical scales reads $\alpha_s(m_H/2) = 0.1251$, $\alpha_s(m_H) = 0.1126$ and $\alpha_s(2m_H) = 0.1024$.

In table 1, we show the different contributions to the decay width $\Gamma_{H \rightarrow b\bar{b}}$ in the $\overline{\text{MS}}$ scheme. The LO and NLO results come only from the C_2C_2 channel. At NNLO, the C_1C_2 channel provides a correction of 0.8%, which is one-fourth of that in the C_2C_2 channel. At NNNLO, the sum of the C_1C_2 and C_1C_1 channels is about five times that of the C_2C_2 channel, signifying the importance of including the top-quark Yukawa contributions. The $\mathcal{O}(\alpha_s^4)$ corrections in the C_2C_2 channel decrease the decay width by 0.1%. In contrast, the $\mathcal{O}(\alpha_s^4)$ corrections in the C_1C_1 channel still enhance the decay width by 0.4%, a magnitude larger than the expected experimental precision (0.21%) at future lepton colliders [4].

$\mu = m_H$	[MeV]	$\Gamma_{Hb\bar{b}}^{C_2C_2}$	$\Gamma_{Hb\bar{b}}^{C_1C_2}$	$\Gamma_{Hb\bar{b}}^{C_1C_1}$
$\Gamma_{H \rightarrow b\bar{b}}(\overline{\text{MS}})$	$\mathcal{O}(\alpha_s^0)$	1.9076	-	-
	$\mathcal{O}(\alpha_s^1)$	0.3873	-	-
	$\mathcal{O}(\alpha_s^2)$	0.0735	0.0183	-
	$\mathcal{O}(\alpha_s^3)$	0.0048	0.0142	0.0090
	$\mathcal{O}(\alpha_s^4)$	-0.0025	*	0.0087

Table 1: Different contributions to the decay width in the $\overline{\text{MS}}$ scheme at $\mu = m_H$. The notation ‘*’ represents a correction which has not been calculated.

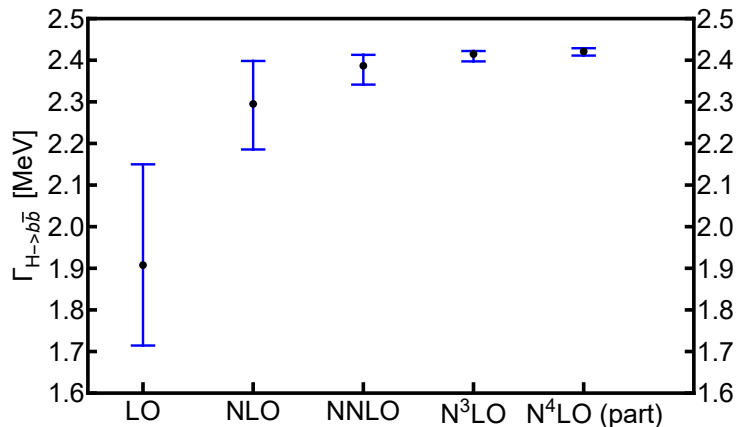


Figure 2: The decay width of $H \rightarrow b\bar{b}$ in the $\overline{\text{MS}}$ scheme at different perturbative orders. The error bar denotes the scale uncertainty.

The scale uncertainty of the decay width is estimated by varying the renormalization scale around its default value m_H by a factor of two. As shown in figure 2, the scale uncertainty is significantly improved, reducing from 0.7% at NNNLO to 0.4% after including the $\mathcal{O}(\alpha_s^4)$ corrections we computed in this work. In addition, the uncertainty from $\delta\alpha_s = 0.0009$ brings an error of 0.2%. Therefore, we obtain

$$\Gamma_{H \rightarrow b\bar{b}}^{\text{N}^4\text{LO QCD}}(\overline{\text{MS}}) = 2.421_{-0.010}^{+0.008}(\text{scl.})_{-0.005}^{+0.005}(\alpha_s) \text{ MeV}. \quad (32)$$

The decay width can be used to derive the value of the bottom quark mass. In figure 3, we show the relation between these two quantities. If the decay width is measured with an

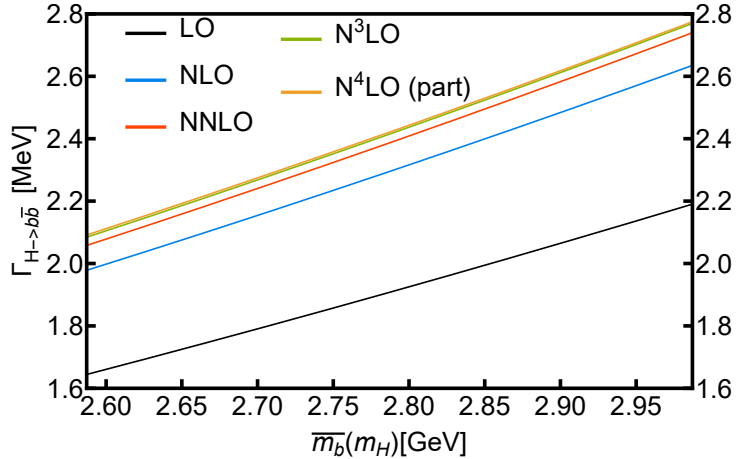


Figure 3: The decay width of $H \rightarrow b\bar{b}$ as a function of the bottom quark mass $\bar{m}_b(m_H)$ that varies from 2.584 GeV to 2.984 GeV.

uncertainty of 0.21% [4], the bottom quark mass can be derived with a precision around 0.36%, where the theoretical uncertainties are taken into account.

5 Conclusion

The decay width of the Higgs boson to bottom quarks is a fundamental quantity that will be precisely measured at future colliders. To match the experimental accuracy, it is essential to provide theoretical predictions with the same or even better precision. We calculate the $\mathcal{O}(\alpha_s^4)$ corrections in the C_1C_1 channel, finding that they increase the decay width by 0.4% and reduce the scale dependence to 0.4%. We also discuss the uncertainty from the strong coupling and present the expected precision of the bottom quark mass derived from the measurements of the decay width at future lepton colliders. The next goal would be the $\mathcal{O}(\alpha_s^4)$ corrections in the C_1C_2 channel in order to provide a theoretical prediction with sufficient accuracy.

Acknowledgements

We thank Dong-Hao Li and Xiaofeng Xu for helpful discussions. This work was supported by the National Natural Science Foundation of China under Nos. 12405117, 12321005, 12375076, 12535006. X.W. is also supported by the University Development Fund of The Chinese University of Hong Kong, Shenzhen, under the Grant No. UDF01003912.

A Topological diagrams of the master integrals

In this appendix, we show the topological diagrams of the master integrals in figure 4.

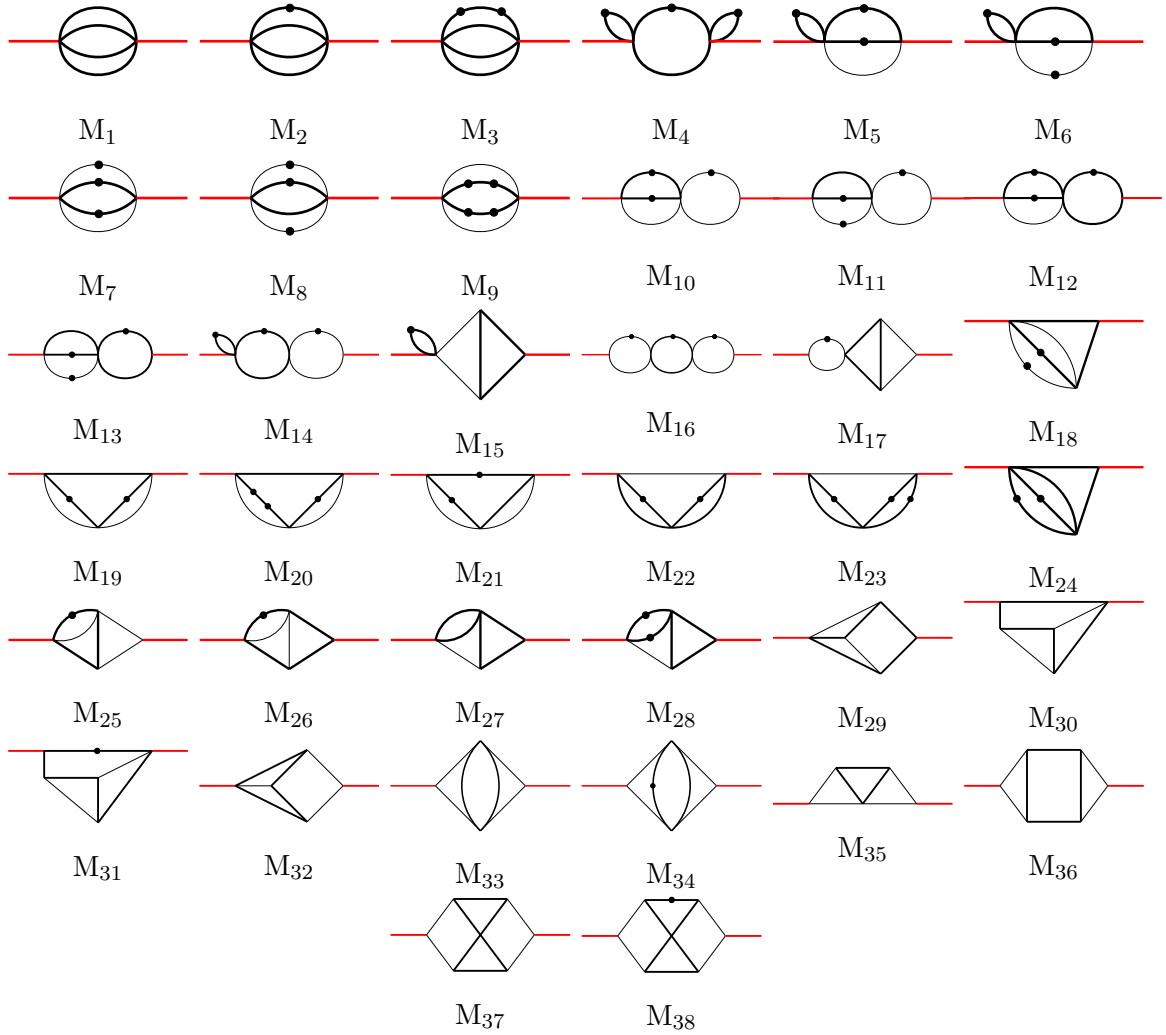


Figure 4: Topological diagrams of the master integrals. The thick black and red lines stand for the massive bottom quark and the Higgs boson, respectively. One black dot indicates one additional power of the corresponding propagator.

References

- [1] ATLAS collaboration, “Projections for measurements of Higgs boson cross sections, branching ratios, coupling parameters and mass with the ATLAS detector at the HL-LHC.” ATL-PHYS-PUB-2018-054, 2018.
- [2] Y. Zhu, H. Cui and M. Ruan, *The Higgs $\rightarrow b\bar{b}, c\bar{c}$, gg measurement at CEPC*, *JHEP* **11** (2022) 100, [2203.01469].
- [3] CEPC PHYSICS STUDY GROUP collaboration, H. Cheng et al., *The Physics potential of the CEPC. Prepared for the US Snowmass Community Planning Exercise (Snowmass 2021)*, in *Snowmass 2021*, 5, 2022, 2205.08553.
- [4] J. Altmann et al., *ECFA Higgs, electroweak, and top Factory Study*, vol. 5/2025 of *CERN Yellow Reports: Monographs*. 6, 2025, 10.23731/CYRM-2025-005.
- [5] E. Braaten and J. P. Leveille, *Higgs Boson Decay and the Running Mass*, *Phys. Rev. D* **22** (1980) 715.

- [6] N. Sakai, *Perturbative QCD Corrections to the Hadronic Decay Width of the Higgs Boson*, *Phys. Rev. D* **22** (1980) 2220.
- [7] P. Janot, *First Order QED and QCD Radiative Corrections to Higgs Decay Into Massive Fermions*, *Phys. Lett. B* **223** (1989) 110–118.
- [8] M. Drees and K.-i. Hikasa, *NOTE ON QCD CORRECTIONS TO HADRONIC HIGGS DECAY*, *Phys. Lett. B* **240** (1990) 455.
- [9] A. Dabelstein and W. Hollik, *Electroweak corrections to the fermionic decay width of the standard Higgs boson*, *Z. Phys. C* **53** (1992) 507–516.
- [10] B. A. Kniehl, *Radiative corrections for $H \rightarrow f \text{ anti-}f (\gamma)$ in the standard model*, *Nucl. Phys. B* **376** (1992) 3–28.
- [11] K. G. Chetyrkin and A. Kwiatkowski, *Second order QCD corrections to scalar and pseudoscalar Higgs decays into massive bottom quarks*, *Nucl. Phys. B* **461** (1996) 3–18, [[hep-ph/9505358](#)].
- [12] R. Harlander and M. Steinhauser, *Higgs decay to top quarks at $O(\alpha_s^2)$* , *Phys. Rev. D* **56** (1997) 3980–3990, [[hep-ph/9704436](#)].
- [13] A. Primo, G. Sasso, G. Somogyi and F. Tramontano, *Exact Top Yukawa corrections to Higgs boson decay into bottom quarks*, *Phys. Rev. D* **99** (2019) 054013, [[1812.07811](#)].
- [14] J. Wang, Y. Wang and D.-J. Zhang, *Analytic decay width of the Higgs boson to massive bottom quarks at next-to-next-to-leading order in QCD*, *JHEP* **03** (2024) 068, [[2310.20514](#)].
- [15] W. Bernreuther, L. Chen and Z.-G. Si, *Differential decay rates of CP-even and CP-odd Higgs bosons to top and bottom quarks at NNLO QCD*, *JHEP* **07** (2018) 159, [[1805.06658](#)].
- [16] A. Behring and W. Bizoń, *Higgs decay into massive b-quarks at NNLO QCD in the nested soft-collinear subtraction scheme*, *JHEP* **01** (2020) 189, [[1911.11524](#)].
- [17] G. Somogyi and F. Tramontano, *Fully exclusive heavy quark-antiquark pair production from a colourless initial state at NNLO in QCD*, *JHEP* **11** (2020) 142, [[2007.15015](#)].
- [18] S. G. Gorishnii, A. L. Kataev, S. A. Larin and L. R. Surguladze, *Corrected Three Loop QCD Correction to the Correlator of the Quark Scalar Currents and γ (Tot) ($H^0 \rightarrow$ Hadrons)*, *Mod. Phys. Lett. A* **5** (1990) 2703–2712.
- [19] K. G. Chetyrkin, *Correlator of the quark scalar currents and $\Gamma(\text{tot})$ ($H \rightarrow$ hadrons) at $O(\alpha_s^3)$ in pQCD*, *Phys. Lett. B* **390** (1997) 309–317, [[hep-ph/9608318](#)].
- [20] P. A. Baikov, K. G. Chetyrkin and J. H. Kuhn, *Scalar correlator at $O(\alpha_s^4)$, Higgs decay into b-quarks and bounds on the light quark masses*, *Phys. Rev. Lett.* **96** (2006) 012003, [[hep-ph/0511063](#)].
- [21] F. Herzog, B. Ruijl, T. Ueda, J. A. M. Vermaseren and A. Vogt, *On Higgs decays to hadrons and the R-ratio at N^4LO* , *JHEP* **08** (2017) 113, [[1707.01044](#)].
- [22] C. Anastasiou, F. Herzog and A. Lazopoulos, *The fully differential decay rate of a Higgs boson to bottom-quarks at NNLO in QCD*, *JHEP* **03** (2012) 035, [[1110.2368](#)].

- [23] V. Del Duca, C. Duhr, G. Somogyi, F. Tramontano and Z. Trócsányi, *Higgs boson decay into b -quarks at NNLO accuracy*, *JHEP* **04** (2015) 036, [1501.07226].
- [24] R. Mondini, M. Schiavi and C. Williams, *N^3LO predictions for the decay of the Higgs boson to bottom quarks*, *JHEP* **06** (2019) 079, [1904.08960].
- [25] X. Chen, P. Jakubčík, M. Marcoli and G. Stagnitto, *The parton-level structure of Higgs decays to hadrons at N^3LO* , *JHEP* **06** (2023) 185, [2304.11180].
- [26] J. Yan, X.-G. Wu, J.-M. Shen, X.-D. Huang and Z.-F. Wu, *Scale-invariant total decay width $\Gamma(H \rightarrow b\bar{b})$ using the novel method of characteristic operator*, *JHEP* **04** (2025) 184, [2411.15402].
- [27] E. Fox, A. Gehrmann-De Ridder, T. Gehrmann, N. Glover, M. Marcoli and C. T. Preuss, *Jet Rates in Higgs Boson Decay at Third Order in QCD*, *Phys. Rev. Lett.* **134** (2025) 251905, [2502.17333].
- [28] A. L. Kataev, *The Order $O(\alpha\alpha_s)$ and $O(\alpha_s^2)$ corrections to the decay width of the neutral Higgs boson to the anti- b b pair*, *JETP Lett.* **66** (1997) 327–330, [hep-ph/9708292].
- [29] L. Mihaila, B. Schmidt and M. Steinhauser, *$\Gamma(H \rightarrow b\bar{b})$ to order $\alpha\alpha_s$* , *Phys. Lett. B* **751** (2015) 442–447, [1509.02294].
- [30] R. Mondini, U. Schubert and C. Williams, *Top-induced contributions to $H \rightarrow b\bar{b}$ and $H \rightarrow c\bar{c}$ at $\mathcal{O}(\alpha_s^3)$* , *JHEP* **12** (2020) 058, [2006.03563].
- [31] J. Wang, X. Wang and Y. Wang, *Analytic decay width of the Higgs boson to massive bottom quarks at order α_s^3* , *JHEP* **03** (2025) 163, [2411.07493].
- [32] J. Wang and Y. Wang, *Analytic result of Higgs boson decay to gluons with full quark mass dependence*, *Phys. Lett. B* **869** (2025) 139865, [2503.22169].
- [33] H. Kluberg-Stern and J. B. Zuber, *Ward Identities and Some Clues to the Renormalization of Gauge Invariant Operators*, *Phys. Rev. D* **12** (1975) 467–481.
- [34] N. K. Nielsen, *Gauge Invariance and Broken Conformal Symmetry*, *Nucl. Phys. B* **97** (1975) 527–540.
- [35] N. K. Nielsen, *The Energy Momentum Tensor in a Nonabelian Quark Gluon Theory*, *Nucl. Phys. B* **120** (1977) 212–220.
- [36] K. G. Chetyrkin, B. A. Kniehl and M. Steinhauser, *Three loop $O(\alpha_s^2 G(F) M(t)^2)$ corrections to hadronic Higgs decays*, *Nucl. Phys. B* **490** (1997) 19–39, [hep-ph/9701277].
- [37] K. G. Chetyrkin, B. A. Kniehl and M. Steinhauser, *Decoupling relations to $O(\alpha_s^3)$ and their connection to low-energy theorems*, *Nucl. Phys. B* **510** (1998) 61–87, [hep-ph/9708255].
- [38] K. G. Chetyrkin, J. H. Kuhn and C. Sturm, *QCD decoupling at four loops*, *Nucl. Phys. B* **744** (2006) 121–135, [hep-ph/0512060].
- [39] T. Liu and M. Steinhauser, *Decoupling of heavy quarks at four loops and effective Higgs-fermion coupling*, *Phys. Lett. B* **746** (2015) 330–334, [1502.04719].
- [40] J. Davies, M. Steinhauser and D. Wellmann, *Completing the hadronic Higgs boson decay at order α_s^4* , *Nucl. Phys. B* **920** (2017) 20–31, [1703.02988].

- [41] T. Hahn, *Generating Feynman diagrams and amplitudes with FeynArts 3*, *Comput. Phys. Commun.* **140** (2001) 418–431, [[hep-ph/0012260](#)].
- [42] A. Alloul, N. D. Christensen, C. Degrande, C. Duhr and B. Fuks, *FeynRules 2.0 - A complete toolbox for tree-level phenomenology*, *Comput. Phys. Commun.* **185** (2014) 2250–2300, [[1310.1921](#)].
- [43] V. Shtabovenko, R. Mertig and F. Orellana, *FeynCalc 9.3: New features and improvements*, *Comput. Phys. Commun.* **256** (2020) 107478, [[2001.04407](#)].
- [44] V. Shtabovenko, R. Mertig and F. Orellana, *FeynCalc 10: Do multiloop integrals dream of computer codes?*, *Comput. Phys. Commun.* **306** (2025) 109357, [[2312.14089](#)].
- [45] F. V. Tkachov, *A Theorem on Analytical Calculability of Four Loop Renormalization Group Functions*, *Phys. Lett. B* **100** (1981) 65–68.
- [46] K. G. Chetyrkin and F. V. Tkachov, *Integration by Parts: The Algorithm to Calculate beta Functions in 4 Loops*, *Nucl. Phys. B* **192** (1981) 159–204.
- [47] J. Klappert, F. Lange, P. Maierhöfer and J. Usovitsch, *Integral reduction with Kira 2.0 and finite field methods*, *Comput. Phys. Commun.* **266** (2021) 108024, [[2008.06494](#)].
- [48] L.-B. Chen, J. Wang and Y. Wang, *Analytic NNLO QCD corrections to top quark pair production in electron-positron collisions*, *JHEP* **09** (2024) 014, [[2405.18912](#)].
- [49] R. N. Lee and A. I. Onishchenko, *ϵ -regular basis for non-polylogarithmic multiloop integrals and total cross section of the process $e^+e^- \rightarrow 2(Q\bar{Q})$* , *JHEP* **12** (2019) 084, [[1909.07710](#)].
- [50] A. V. Kotikov, *Differential equation method: The Calculation of N point Feynman diagrams*, *Phys. Lett. B* **267** (1991) 123–127.
- [51] J. M. Henn, *Multiloop integrals in dimensional regularization made simple*, *Phys. Rev. Lett.* **110** (2013) 251601, [[1304.1806](#)].
- [52] A. B. Goncharov, *Multiple polylogarithms, cyclotomy and modular complexes*, *Math. Res. Lett.* **5** (1998) 497–516, [[1105.2076](#)].
- [53] H. Ferguson, D. Beiley and S. Arno, *Analysis of PSLQ, an integer relation finding algorithm*, *Math. Comp.* **68** (1999) 351.
- [54] X. Liu, Y.-Q. Ma and C.-Y. Wang, *A Systematic and Efficient Method to Compute Multi-loop Master Integrals*, *Phys. Lett. B* **779** (2018) 353–357, [[1711.09572](#)].
- [55] X. Liu, Y.-Q. Ma, W. Tao and P. Zhang, *Calculation of Feynman loop integration and phase-space integration via auxiliary mass flow*, *Chin. Phys. C* **45** (2021) 013115, [[2009.07987](#)].
- [56] X. Liu and Y.-Q. Ma, *AMFlow: A Mathematica package for Feynman integrals computation via auxiliary mass flow*, *Comput. Phys. Commun.* **283** (2023) 108565, [[2201.11669](#)].
- [57] Z.-F. Liu and Y.-Q. Ma, *Determining Feynman Integrals with Only Input from Linear Algebra*, *Phys. Rev. Lett.* **129** (2022) 222001, [[2201.11637](#)].
- [58] J. Wang, X. Wang and Y. Wang. To appear.
- [59] ϵ -COLLABORATION collaboration, I. Bree et al., *The geometric bookkeeping guide to Feynman integral reduction and ϵ -factorised differential equations*, [2506.09124](#).

- [60] I. Bree et al., *New algorithms for Feynman integral reduction and ε -factorised differential equations*, 2511.15381.
- [61] PARTICLE DATA GROUP collaboration, S. Navas et al., *Review of particle physics*, *Phys. Rev. D* **110** (2024) 030001.
- [62] ATLAS, CMS collaboration, G. Aad et al., *Combined Measurement of the Higgs Boson Mass in pp Collisions at $\sqrt{s} = 7$ and 8 TeV with the ATLAS and CMS Experiments*, *Phys. Rev. Lett.* **114** (2015) 191803, [1503.07589].
- [63] K. G. Chetyrkin, J. H. Kuhn and M. Steinhauser, *RunDec: A Mathematica package for running and decoupling of the strong coupling and quark masses*, *Comput. Phys. Commun.* **133** (2000) 43–65, [hep-ph/0004189].
- [64] F. Herren and M. Steinhauser, *Version 3 of RunDec and CRunDec*, *Comput. Phys. Commun.* **224** (2018) 333–345, [1703.03751].